Comparing the performance of RANS turbulence models between different cavity flow benchmarks

Elyas Larkermani[1*], *Vegard* Mikkelsen Bjerkeli[1], and *Laurent* Georges[1]

[1]Norwegian University of Science and Technology, Department of Energy and Process Engineering, Kolbjørn Hejes v 1B, NO-7491, Trondheim, Norway

Abstract. To evaluate the performance of RANS turbulence models, this study compares four different cavity flow benchmarks using the prevailing two-equation turbulence models for indoor airflows, namely the standard and RNG k-ε and the standard and SST k-ω models. A cavity flow consists of one air inlet and one outlet slot. The inlet slot is positioned on the upper left corner of the cavity, whereas the outlet slot is located in the lower right. This cavity flow is representative of mixing ventilation. These four cavity benchmarks differ by their geometry (i.e., the aspect ratio of the room), flow regime and whether the flow is isothermal or not. Measurements of the air velocity and temperature in these benchmarks are used to evaluate the accuracy of the RANS turbulence models. Many existing studies have investigated the airflow and heat transfer over these benchmarks. However, the numerical methods and other relevant CFD parameters are not always described in detail, reducing the transparency and reproducibility of these works. To compare the influence of the RANS turbulence model on the four cavity flows, a same CFD setup is adopted here for all benchmarks. This setup is based on the best practice in RANS, namely a steady second-order spatial discretization on a wall-resolved structured mesh and with a grid convergence analysis. The results show that k-ε models, particularly the standard k-ε model, are best suited in a fully turbulent flow regime without strong pressure gradients. On the opposite, the SST k-ω model performs best in the transitional regime while the k-ε models only give moderate to poor results.

1 Introduction

Accurate prediction of indoor airflows is required to design comfortable and healthy indoor environments. Designers may use indoor flow modeling to evaluate the proposed ventilation strategy and ensure that the thermal comfort and indoor air quality (IAQ) criteria are met at the design stage. However, it should deliver sufficiently accurate detail at a low financial and labor cost. The two most common approaches that have been developed to study indoor airflow are experimental measurements and computational fluid dynamics (CFD). The former approach is usually implemented on the full scale of the actual model. However, reliable and detailed information on indoor airflows can be provided at a lower cost using CFD. Substantial development in numerical schemes, turbulence models, and computational power make CFD more efficient today than 50 years ago. Although some measurement techniques are still in use and essential to validate CFD simulations, CFD can replace some of these flow measurements to reduce the costs.

The Reynolds-Averaged Navier Stokes (RANS) turbulence modeling is widely used to simulate airflows in ventilated spaces. Other approaches such as Large Eddy Simulation (LES) are more accurate for ventilation flow prediction, but their applications are quite limited due to higher computational costs. However, three distinct physical phenomena of indoor airflows, i.e., transitional flow, turbulence anisotropy and adverse pressure gradients, are demanding for RANS modeling [1]. The performance of many RANS turbulence models may change significantly depending on the flow regime. Although a fully turbulent airflow develops in the room, a transitional airflow may still form in some regions, e.g., near supply jet or low-velocity regions. In addition, only a few RANS models can capture turbulent anisotropy present in regions of high shear. On top of that, the separation of a boundary layer due to an adverse pressure gradient is not easily predicted with high-Reynolds RANS turbulence models. Therefore, it is uncertain which RANS models are suitable depending on the airflow characteristics in the enclosure.

In two recent studies by Peng et al. [2] and van Hoff et al. [3], the accuracy of CFD simulations for indoor airflows in isothermal and non-isothermal backward facing step flow was evaluated by different teams from the ventilation research community and industry. A large spread in the results was reported during these workshops as multiple user decisions affect the final results, such as the choice of the numerical method. However, the choice of turbulence model was recognized as the parameter with the most significant impact. The results from the two studies indicate the importance of validation against benchmark test cases

* Corresponding author: elyas.larkermani@ntnu.no

with available experimental data to ensure accuracy of CFD simulations for indoor airflows. Our study evaluates the performance of RANS two-equation eddy-viscosity models in four different cavity flow benchmarks representative for mixing ventilation at both transitional and fully turbulent regimes.

2 Methodology

2.1 Description of the cavity flow benchmarks

A cavity flow represents an airflow in an empty ventilated space where an attached wall jet is discharged into the room along the ceiling. With a sufficiently high inlet velocity, the jet impinges the opposing wall and deflects into the cavity zone. The separation of the boundary layer close to the top corner of the room generates a recirculation region in the enclosure (Figure 1). The four cavity flows differ by the geometry aspect ratio, the airflow regime and thermal effects (i.e., isothermal and non-isothermal cases). The first benchmark called the IEA Annex 20 test room is isothermal. The experimental measurements were carried out by Nielsen et al. [4] using Laser Doppler Anemometry (LDA). The slot Reynolds number (Re) is 5000, indicating a fully turbulent room airflow. Since its creation, multiple attempts [5-9] have been made to reproduce the airflow pattern and velocity profile of this cavity flow using the prevailing turbulence models for indoor airflows such as k-ε, RNG k-ε, k-ω and k-ω SST. The dimension of the computational domain is defined in Table 1.

Benchmark 2 has a same geometry as benchmark 1 but with a different aspect ratio (Table 1). The experimental data are reported by Nielsen [10] in his Ph.D. thesis for both isothermal and non-isothermal conditions. The isothermal flow was measured with hot wire anemometry, and measurements were done only at a vertical line $(x = 2H)$. The benchmark is simulated here for a Reynolds number of 7100 in isothermal mode.

In benchmark 3, a slightly different geometrical configuration compared to benchmarks 1 and 2 is adopted as the width is considerably smaller than the length and height (Table 1). So inlet and outlet openings have a smaller area than the previous ones. The flow is non-isothermal. In the experiments done by Blay et al. [11], the setup has two guard cavities to make the side walls adiabatic. The walls were made of aluminum and kept at a constant temperature using temperature-controlled water (with a precision of 0.25°C). The floor is kept at a constant temperature of 35.5°C, while the remaining three walls have a temperature equal to the inlet temperature of 15°C. A uniform velocity profile of 0.57 m/s is imposed at the inlet, leading to a Reynolds number of 684 based on the inlet height. Velocity measurements were done using Laser Doppler Velocimetry (LDV) and temperature measurements with Cr-Al thermocouples.

Benchmark 4 is a cubical cavity without buoyancy effects (Table 1). The experiment was done by van Hoff et al. [12] at two different Reynolds numbers, 1000 and 2500, representing a transitional flow. The working fluid was water, and the velocity field was measured with a 2D PIV system.

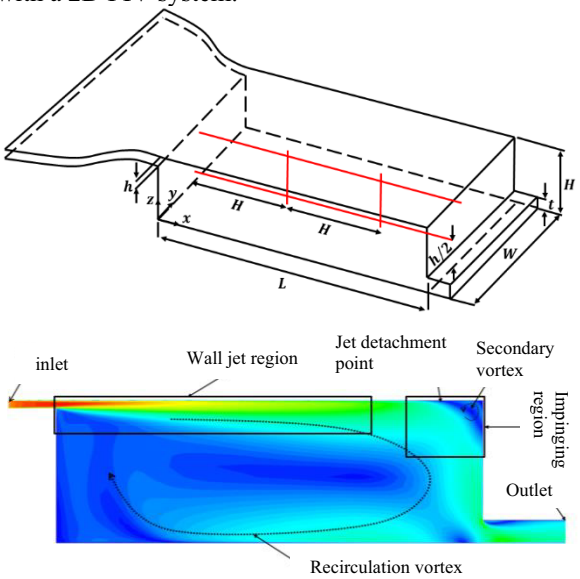

Fig. 1. IEA Annex 20 test room [4]. The measurement lines in benchmarks 1 and 2 are two vertical lines and two horizontal lines in red.

Table 1. Cavity flow benchmark description.

Benchmark	1	2	3	4
Re at inlet	5000	7100	684	1000/2500
Flow regime	Fully Turbulent	Fully Turbulent	Unknown	Transitional
Thermal effects	Isothermal	Isothermal	Non-Isothermal	Isothermal
L/H	3	3	1	1
W/H	1	4.7	0.288	1
h/H	0.056	0.056	0.0173	0.1
t/H	0.16	0.16	0.0231	0.0167
H [m]	0.0893	0.127	1.04	0.3

2.2 Governing equations and numerical setup

The airflow field in a cavity is computed using the Reynolds Averaged Navier-Stokes (RANS) equations for the mass, momentum and energy conservations where the Reynolds stresses have been modeled using an eddy viscosity:

$$\frac{\partial \bar{u}_i}{\partial x_i} = 0 \tag{1}$$

$$\frac{\partial \bar{u}_i}{\partial t} + \frac{\partial \bar{u}_i \bar{u}_j}{\partial x_j} = -\frac{1}{\rho_{\text{ref}}}\frac{\partial \bar{p}}{\partial x_i} + \frac{\partial}{\partial x_j}\left[(\upsilon + \upsilon_t)\frac{\partial \bar{u}_j}{\partial x_j}\right] + \beta g_i(\bar{T} - T_{\text{ref}}) \tag{2}$$

$$\frac{\partial \bar{T}}{\partial t} + \frac{\partial \bar{u}_j \bar{T}}{\partial x_j} = \frac{\partial}{\partial x_j}\left[(\alpha + \alpha_t)\frac{\partial \bar{T}}{\partial x_j}\right] \tag{3}$$

where the bar represents the time averaging, x_i denotes the i^{th} spatial coordinate direction, $\bar{u}_i$ represents the time-averaged velocity field in the x_i direction, t the time, $\bar{p}$ the time-averaged static pressure, and $\bar{T}$ the time-averaged temperature. The effect of buoyancy forces is taken into account using the Boussinesq

approximation where $\beta = 1/T_{\text{ref}}$ is the thermal expansion coefficient of the air modeled as an ideal gas and g_i the gravitational acceleration. The parameters υ and α are the kinematic viscosity and thermal diffusivity, respectively. Turbulent kinematic viscosity and thermal diffusivity are defined with the subscript *t*.

After conducting a grid sensitivity analysis for each benchmark, a structured orthogonal mesh is selected based on a trade-off between accuracy and computational cost. An overview of the grid size adopted for each benchmark is provided in Table 2. All meshes have been constructed to have y^+ less than five on the walls to resolve the boundary layers. The turbulence model that showed good convergence in previous studies is selected for grid analysis. The inlet turbulent intensity is set to match the experimental value.

Table 2. Grid size based on grid sensitivity analysis.

Benchmark	1	2	3	4
Geometry	3D	3D	3D	3D
Number of cells	342000	1771000	189000	1214000
Inlet turbulent intensity	4%	5%	6%	6%
Turbulence model	Standard $\mathbf{k-\varepsilon}$	Standard $\mathbf{k-\varepsilon}$	RNG $\mathbf{k-\varepsilon}$	SST $\mathbf{k-\omega}$

The nonlinear governing equations are discretized using a second-order cell-centered finite volume method implemented in the ANSYS Fluent commercial CFD package. The SIMPLE algorithm is employed for pressure-velocity coupling. The time derivatives are advanced in time using the "Second Order Implicit" scheme. The "Second Order Upwind" scheme is adopted for the treatment of the convective terms of the governing equations. The pressure interpolation is provided by the "Second Order" scheme. "Enhanced wall treatment" has been used as the default wall modeling option. The no-slip boundary condition is applied to all walls.

All benchmarks are run in steady-state mode. However, the averaging technique introduced by Blocken [13] is applied when fluctuations of the residuals and other physical quantities (such as the drag coefficients on the floor or ceiling) are detected. In this technique, the solution is averaged over many iterations to get a statistically independent solution. The number of iterations required is case dependent and must be investigated for each benchmark. The convergence criteria for all simulations are fulfilled when the absolute residuals drop down to 10^{-6} and the drag coefficient on the ceiling and floor walls reaches stable values.

3 Results and discussion

The performance of six turbulence models, the standard k-ε, RNG k-ε, realizable k-ε, AKN low-Re k-ε, standard k-ω and the k-ω SST, is shown for the four benchmarks in Figures 2 and 3.

3.1 Benchmarks 1 and 2

The distribution of the normalized streamwise velocity component along the cavity height at two vertical lines ($x = H,\ x = 2H$) is plotted in Figures 2(a), (b), (e) and (f). The negative velocities in the lower part of the cavity are evidence of a substantial air recirculation region inside the cavity. Figures 2(c), (d), (g) and (h) show normalized vertical velocity distribution along two horizontal lines ($z = h/2,\ z = H - h/2$) in the mid-plane. None of the turbulence models achieves a perfect fit of the experimental data. In particular, in Figure 2(c), simulation results differ remarkably from experiments. From this figure, the RNG and realizable k-ε turbulence models cannot correctly predict the flow direction on the cavity's left part. In other words, solutions from these models have a different flow pattern than experiments in this part of the cavity. The most apparent differences between the turbulence models can also be found in the lower-left corner of the cavity, i.e., the left part of Figures 2(c) and (g). Turbulence models struggle to model the flow in this part of the cavity because the flow may be dominated by the transitional regime and have anisotropic behavior. Figures 2(a) and (b) also reveal a noticeable deviation between the turbulence models regarding the jet velocity along the floor and ceiling.

3.2 Benchmark 3

Profiles of normalized velocity and temperature along a vertical centerline ($x = L/2$) are depicted in Figures 2(i) and (j) as well as along a horizontal centerline ($z = H/2$) in Figures 2(k) and (l). Since simulations gave oscillatory residuals, the results were averaged over 2000 iterations for each model. According to Figures 2(i) to (l), all turbulence models predict fairly accurately the flow pattern. However, the maximum velocity for the jet along the ceiling is overestimated by two k-ω models. Moreover, all models underestimate the jet velocity along the floor and left wall under the inlet. Although the air temperature along the cavity walls is in good agreement with measurement data, it is underpredicted by all models inside the recirculation zone due to insufficient air mixing (Figures 2(j) and (l)). The realizable k-ε model reproduces experiment data better than other turbulence models, whereas the k-ω SST model is relatively less successful.

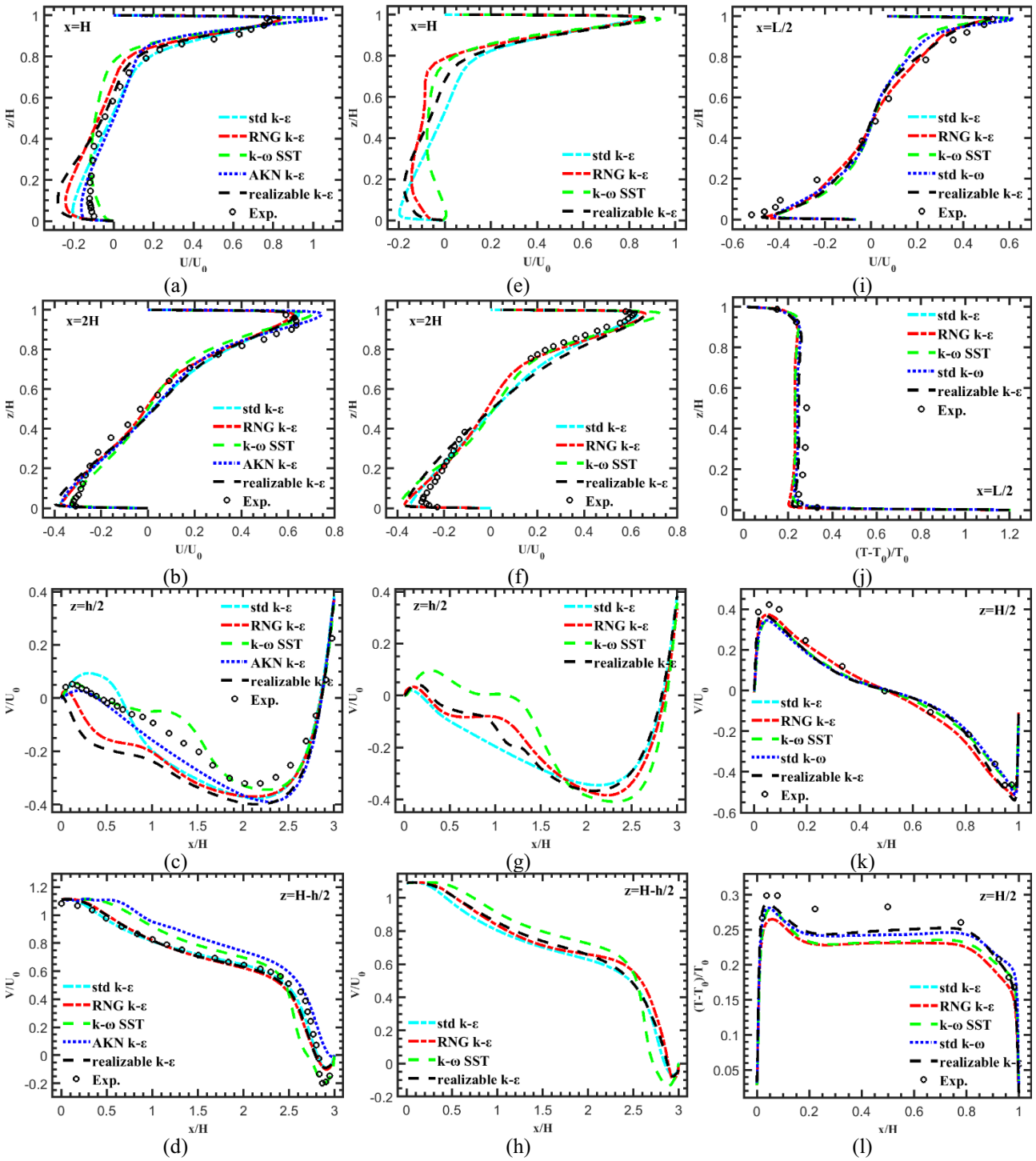

Fig. 2. Normalized velocity and temperature profiles for benchmark 1 (left column), benchmark 2 (middle column) and benchmark 3 (right column)

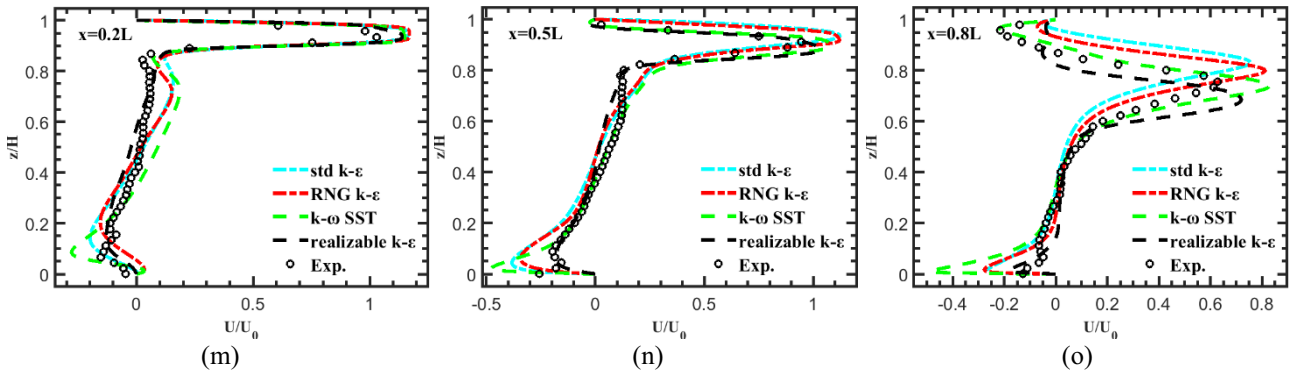

Fig. 3. Normalized velocity and temperature profiles for benchmark 4

3.3 Benchmark 4

Normalized velocity profiles from standard k-ε, RNG k-ε, realizable k-ε, and k-ω SST turbulence models at three vertical lines ($x = 0.2L, 0.5L, 0.8L$) are compared with the experimental results in Figures 3(m) to 3(o). Using the k-ω SST model, the location of the detachment of the jet can be predicted quite well (Figure 3(o)). The other models predict detachment further away from the inlet. Right above the floor, a large discrepancy with measurement data can be observed in the velocity profile at all three lines. However, no conclusion can be drawn due to reflections from the glass floor leading to inaccurate measurements. For all three lines, each model appears to overpredict the maximum jet velocity. The k-ω SST shows the best performance, while the standard k-ε has the largest deviation from experiments.

3.4 Cross comparison

It can be concluded that none of the turbulence models perform equally well for all benchmarks, so none of the models seem universal. The main conclusions are:

- Generally, a good agreement is found between CFD results and measurements that validate the use of CFD for the prediction of airflows in buildings.
- The standard k-ε model is the most accurate for benchmarks 1 and 2. In addition, the results obtained using the standard k-ε model are consistent with the literature. The standard k-ε model is thus a good choice when simulating indoor airflows with fully turbulent characteristics without large pressure gradients.
- The deviation from the experimental measurements in the area below the inlet in benchmarks 1 and 2 may be attributed to the anisotropy of the transitional flow present in that region because RANS eddy-viscosity models cannot be taken into account the flow anisotropy.
- All three k-ε models provided the best agreement with experiments in benchmark 3, whereas the k-ω SST model was clearly superior to the k-ε models for benchmark 4. Benchmark 4 has larger pressure gradients along the wall jet. The poor results of k-ε models are primarily caused by an incorrect determination of the location of jet detachment, so they should be used with caution for transitional flows. The standard k-ε model gave the worst results. The k-ω SST model performs better in the transitional flow regime with pressure gradients and jet impingement.

4 Conclusions

In this study, the performance of the prevalent two-equation RANS turbulence models to predict mixing ventilation was studied. The performance was compared with experimental measurements on four cavity flow benchmarks using the CFD best practice. In conclusion, none of the turbulence models performs equally well in all scenarios, confirming the importance of selecting a suitable turbulence model for a given case, e.g., according to the flow regime. Additional benchmarks are needed to discriminate clearly the specific influence of other parameters on the CFD solution, such as the inlet boundary conditions. A similar study using the Large Eddy Simulation (LES) could also be performed to test the universality of LES to accurately predict the indoor airflow characteristics at different flow regimes.

References

1. T. van Hooff, B. Blocken, and G. Van Heijst, “On the suitability of steady RANS CFD for forced mixing ventilation at transitional slot Reynolds numbers,” Indoor Air, **23**, no. 3, pp. 236-249, (2013).
2. L. Peng, P. V. Nielsen, X. Wang, S. Sadrizadeh, L. Liu, and Y. Li, “Possible user-dependent CFD predictions of transitional flow in building ventilation,” Building and Environment, **99**, pp. 130-141, (2016).
3. T. van Hooff, P. V. Nielsen, and Y. Li, “Computational fluid dynamics predictions of non‐isothermal ventilation flow—How can the user factor be minimized?,” Indoor Air, **28**, no. 6, pp. 866-880, (2018).
4. P. V. Nielsen, “Specification of a two-dimensional test case:(iea),” (1990).
5. N. Vogl and U. Renz, “Energy Conservation in Buildings and in Community Systems,” (1991).
6. Q. Chen, “Comparison of different k-ε models for indoor air flow computations,” Numerical Heat Transfer, Part B Fundamentals, **28**, no. 3, pp. 353-369, (1995).
7. Q. Chen, “Prediction of room air motion by Reynolds-stress models,” Building and environment, **31**, no. 3, pp. 233-244, (1996).
8. L. Voigt, “Navier-Stokes simulations of airflow in rooms and around a human body. (2001),” Technical University of Denmark.
9. L. Rong and P. V. Nielsen, “Simulation with different turbulence models in an annex 20 room benchmark test using Ansys CFX 11.0,” (2008).
10. P. V. Nielsen, “Flow in air conditioned rooms: Model experiments and numerical solution of the flow equations,” (1974).
11. D. Blay, “Confined turbulent mixed convection in the presence of horizontal buoyant wall jet,” HTD **213**, Fundamentals of Mixed Convection, (1992).
12. T. van Hooff, B. Blocken, T. Defraeye, J. Carmeliet, and G. Van Heijst, “PIV measurements of a plane wall jet in a confined space at transitional slot Reynolds numbers,” Experiments in Fluids, **53**, no. 2, pp. 499-517, (2012).
13. B. Blocken, “Computational Fluid Dynamics for urban physics: Importance, scales, possibilities, limitations and ten tips and tricks towards accurate and reliable simulations,” Building and Environment, **91**, pp. 219-245, (2015).